Iterative Detection and Decoding for Spatially Coupled Multiuser Data Transmission

Xiaodan Wang(✉), Sijie Wang, Zhongwei Si,
Zhiqiang He, Kai Niu, and Chao Dong

Key Laboratory of Universal Wireless Communications, Ministry of Education,
Beijing University of Posts and Telecommunications, Beijing 100876, China
xiaodanwang@bupt.edu.cn

Abstract. Non-orthogonal multiple access (NOMA) is a candidate multiple access scheme for 5G wireless communication. In this paper we consider applying the principle of spatially coupling in a NOMA system, where coupled data streams from different users transmit via the additive white Gaussian noise (AWGN) multiple access channel. A data stream is constructed by replicating each encoded bit for several times and then permuting the replicated bits. We propose an message-passing algorithm (MPA) based iterative multiuser detection combining with channel decoding, which is illustrated and analysed by the factor graph representation and the extrinsic information transfer (EXIT) chart, respectively. Numerical results show that lower node degree of the spatially coupled structure, higher number of iterations of the detector, and an appropriate encoding/decoding scheme jointly contribute to a better performance of the multiuser transmission system.

Keywords: NOMA · Spatially coupling · Message-passing · Iterative · Detection and decoding

1 Introduction

Different orthogonal multiple access (OMA) schemes have been applied in current wireless communication networks. However, due to the increasing demand of mobile Internet, the 5th generation (5G) wireless communication is required to support massive connectivity of users and/or devices. In a non-orthogonal multiple access (NOMA) system, signals from different users are allowed to be superimposed in the time/frequency resource [1,2]. Therefore, NOMA has gained much attention as a key technique for 5G due to its higher spectral efficiency comparing to OMA.

The technique of spatial graph coupling was first discovered for convolutional low-density parity-check (LDPC) codes [3] and proved to achieve the same limits as the optimum maximum likelihood (ML) decoding [4]. The concept has attracted considerable interests from the area of iterative processing and found applications in many areas of communication including compressive sensing [5], quantum coding [6] and multiuser data transmission [7].

Q. Chen et al. (Eds.): ChinaCom 2016, Part I, LNICST 209, pp. 221–231, 2018.
DOI: 10.1007/978-3-319-66625-9_22

Applying spatial graph coupling to multiple access communication, a sequence of coupled symbols at the transmitter is formed as the sum of equal-power data streams from different users. A data stream is constructed by replicating each encoded bit for several times and then permuting the replicated bits. The data coupling is accomplished by a linear superposition of data streams (in the real or complex domain) from different users transmitted with time offsets. The interconnection of the coupled symbols and the data bits can be described by means of a factor graph [9]. It has been demonstrated in [8] that the system with spatial coupling can achieve the capacity of AWGN multiple access channel even for the case that all the users transmit with equal power and equal rate.

The receiver discussed in [8], which combines minimal-mean squared error (MMSE) with successive interference cancellation (SIC), is capacity-approaching in theory. However, the same performance cannot be achieved in practice since Gaussian assumptions are not appropriate when the number of users is small, and error propagation is inevitable in the SIC. Thus the iterative receiver based on belief propagation (BP) [7,10,11], which is also known as message-passing algorithm (MPA), turns out to be a candidate receiver applied for the multiuser detection in this paper.

Joint multiuser detection and decoding (JMUDD) proposed in [12] is an MPA based receiver. However, the optimization of its joint sparse graph needs complex calculation; otherwise the performance of the receiver may not be satisfying, for example, when using regular LDPC code. In this paper, we focus on the iterative detection and decoding for spatially coupled multiuser data transmission instead of JMUDD. With the help of EXIT chart [13], we investigate the spatially coupling structure and analyse the system performance by varying the number of inner iterations of the detector (and the LDPC decoder) and the outer iterations between the detector and the decoder, as well as the encoding schemes.

The rest of the paper is organized as follows. The system model of the spatially coupled structure is described in Sect. 2. Section 3 introduces the factor graph representation to illustrate corresponding structure and the EXIT chart to analyse the iterative process between the detector and decoders. EXIT chart analysis and numerical results are given in Sect. 4. Section 5 concludes the paper.

2 System Model

We consider a spatially coupling system based on the model of the generalized modulation [14], in which the signal transmitted over the channel is formed by a superposition of different data streams, and each stream contains several data packets.

The data coupling of L users is shown as in Fig. 1. Take the lth user as the example, where $l \in \{1, 2, \ldots, L\}$. First the P packets of the binary information sequence $\mathbf{x}_l = \left[\mathbf{x}_{l,0}^T, \mathbf{x}_{l,1}^T, \ldots, \mathbf{x}_{l,P-1}^T\right]^T$ are fed into a binary channel encoder of code rate $R = K/N$, respectively, where $\mathbf{x}_{l,p} = [x_{l,p,0}, x_{l,p,1}, \ldots, x_{l,p,K-1}]^T$, and $p \in \{0, 1, \ldots, P-1\}$. Without loss of generality, BPSK will be used as

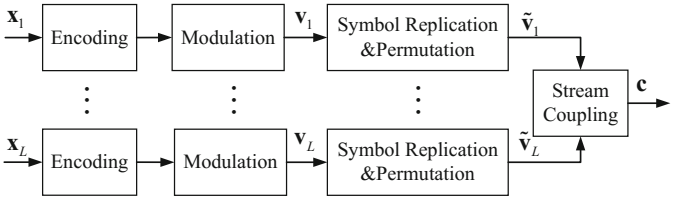

Fig. 1. Block diagram of the coupled signal generation for L users.

the modulation scheme in this paper. Then each packets of the modulated sequence $\mathbf{v}_l = \left[\mathbf{v}_{l,0}^T, \mathbf{v}_{l,1}^T, \ldots, \mathbf{v}_{l,P-1}^T\right]^T$, where $\mathbf{v}_{l,p} = [v_{l,p,0}, v_{l,p,1}, \ldots, v_{l,p,N-1}]^T$, is replicated M times and the symbols in different packets are permuted by different interleavers, producing the transmitting packets of the lth user $\left\{\tilde{\mathbf{v}}_{l,0}^{(0)}, \tilde{\mathbf{v}}_{l,0}^{(1)}, \ldots, \tilde{\mathbf{v}}_{l,0}^{(M-1)}, \ldots, \tilde{\mathbf{v}}_{l,P-1}^{(0)}, \ldots, \tilde{\mathbf{v}}_{l,P-1}^{(M-1)}\right\}$. Finally the coupled signal to be transmitted $\mathbf{c}$ is the superposition of the data packets of different users.

Without loss of generality, we assume that each user utilizes two streams to transmit his data packets in this paper. The process of stream coupling is realized as follows. At time $t = 0$, the first user starts to transmit his first 2 packets, then after a delay of τ symbol intervals the second user joins the transmission. At time $t = 2\tau$, the third user joins and so on. Thus there will be $J = 2L$ modulated data streams overlapping with time offsets. This process is illustrated in Fig. 2 for the case $M = 3$ and $J = 6$ where each row stands for one data stream, and $\tilde{\mathbf{v}}_{l,p}^{(m)}$ denotes the mth replica of $\mathbf{v}_{l,p}$ permuted by the interleaver $\boldsymbol{\pi}_{l,p}^{(m)}$, namely, $\tilde{\mathbf{v}}_{l,p}^{(m)} = \boldsymbol{\pi}_{l,p}^{(m)}\mathbf{v}_{l,p}$ where $m \in \{0, 1, \ldots . M-1\}$. In each data stream a transmitted packet is immediately followed by the next packet. The total transmit data rate equals $RJ/M = \alpha R$ information bits per channel use, where $\alpha = J/M$ is called the modulation load.

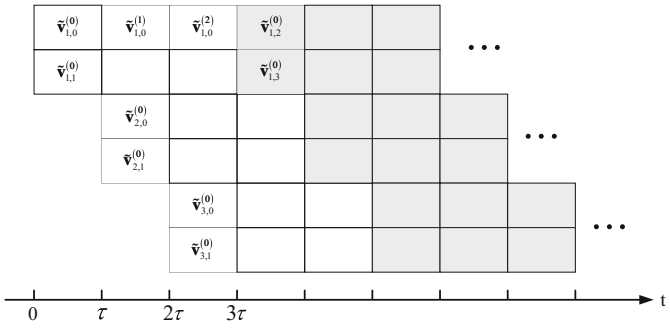

Fig. 2. Coupling process of data streams for different users in the channel. In this case each packet is replicated $M = 3$ times and there are $L = 3$ users with $J = 6$ data streams in total.

The procedure above can be described by an (M, J)-spatially coupling matrix $\mathbf{H}$ as given in (1) on the top of the next page, where $\boldsymbol{\pi}_{l,p}^{(m)}$ is one permutation of the $\tau \times \tau$ identity matrix.

We consider the transmission over an AWGN channel. The received signal can be represented as (2).

$$\mathbf{H} = \begin{bmatrix} \boldsymbol{\pi}_{1,0}^{(0)} & \cdots & \boldsymbol{\pi}_{1,0}^{(M-1)} & \cdots\cdots & \boldsymbol{\pi}_{1,P-2}^{(0)} & \cdots & \boldsymbol{\pi}_{1,P-2}^{(M-1)} & & \\ \boldsymbol{\pi}_{1,1}^{(0)} & \cdots & \boldsymbol{\pi}_{1,1}^{(M-1)} & \cdots\cdots & \boldsymbol{\pi}_{1,P-1}^{(0)} & \cdots & \boldsymbol{\pi}_{1,P-1}^{(M-1)} & & \\ & \boldsymbol{\pi}_{2,0}^{(0)} & \cdots & & \cdots\cdots & & \cdots & \boldsymbol{\pi}_{2,P-2}^{(M-1)} & \\ & \boldsymbol{\pi}_{2,1}^{(0)} & \cdots & & \cdots\cdots & & \cdots & \boldsymbol{\pi}_{2,P-1}^{(M-1)} & \\ & & \ddots & & & \ddots & & & \ddots \\ & & & \boldsymbol{\pi}_{L,0}^{(0)} & \cdots & \cdots\cdots & & \cdots & \boldsymbol{\pi}_{L,P-1}^{(M-1)} \\ & & & \boldsymbol{\pi}_{L,1}^{(0)} & \cdots & \cdots\cdots & & \cdots & \boldsymbol{\pi}_{L,P-1}^{(M-1)} \end{bmatrix} \tag{1}$$

$$\mathbf{y} = \sqrt{\frac{Q}{J}}\mathbf{c} + \mathbf{n}, \tag{2}$$

where $\mathbf{c} = \mathbf{H}^T\mathbf{v}$ is the coupled signal with

$$\begin{aligned} \mathbf{v} = \big[&\mathbf{v}_{1,0}^T, \mathbf{v}_{1,1}^T, \ldots, \mathbf{v}_{L,0}^T, \mathbf{v}_{L,1}^T, \ldots, \\ &\mathbf{v}_{1,P-2}^T, \mathbf{v}_{1,P-1}^T, \ldots, \mathbf{v}_{L,P-2}^T, \mathbf{v}_{L,P-1}^T\big]^T, \end{aligned} \tag{3}$$

and $\mathbf{n}$ is the additive white Gaussian noise with variance σ^2.

Note that the coupled signal $\mathbf{c}$ is multiplied by the power normalizing amplitude $\sqrt{Q/J}$, where $Q = 1$ is the constraint power.

3 Iterative Multiuser Detection and Decoding

In this section, the factor graph representation will be introduced to give more insight details into the spatially coupling structure. Then an iterative MPA-based detection algorithm is applied to accomplish the multiuser detection effectively combining with channel decoding. Furthermore, we briefly introduce EXIT chart which can be utilized to track the exchanging of mutual information at each iteration between the detector and the decoders.

3.1 Factor Graph Representation

The coupling process in the previous section can be illustrated by a factor graph. As shown in Fig. 3, each encoded bit $v_{l,n}$ where $l \in \{1, 2, \ldots, L\}$, $n \in \{0, 1, \ldots, PN-1\}$, corresponds to a variable node represented by a circle, whereas each coupled symbol c_t, $t \in \{0, 1, 2, \ldots\}$ is denoted by a square

called channel node. To be specific, in Fig. 3 there are $L = 2$ users with data bits encoded independently.

An edge connects a variable node to a channel node in the factor graph if that encoded bit is added to the coupled symbol correspondingly. Thus there is a one-to-one correspondence between a factor graph and a spatially coupling matrix. In other words, the number of edges connecting the channel nodes and the variable nodes is equal to the number of 1s in the spatially coupling matrix.

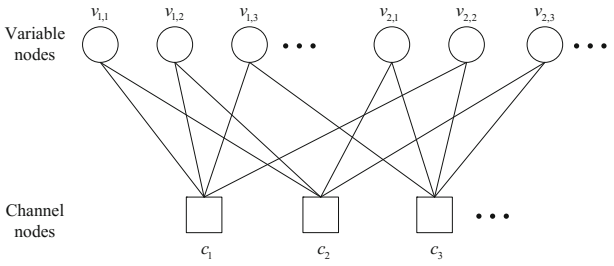

Fig. 3. Factor graph representation for a spatially coupled multiple access system of $L = 2$ users, where channel node degree is 4 and variable node degree is 2.

Define the degree of a node as the number of edges the node connected to other kinds of nodes, thus for the (M, J)-spatially coupled structure, the degrees of the variable nodes and the channel nodes are M and J, respectively.

3.2 Iterative Detection and Decoding Based on MPA

In this subsection, the process of iterative detection and decoding based on MPA is introduced, where the detector exchanges the extrinsic message with the decoders of different users. First, the variable nodes exchange the extrinsic information with the channel nodes inside the detector using *a priori* information which has been received from the corresponding decoders. Then based on the received *a priori* information from the detector, the decoders update the extrinsic information which will be passed to the detector for the next iteration. Define the inner iteration as the message passing process inside the detector or the decoder, while the outer iteration as the message passing process between them. The log-likelihood ratios (LLRs) of the inner iteration and the outer iteration can be calculated as follows.

Inner Iterations of the Detector. During each iteration inside the detector, the extrinsic messages is exchanged between the channel nodes and the variable nodes. Note that the information received from one edge cannot be used to update the information to be transmitted onto that edge. Let the subset $\partial(l, n) \backslash t$ denote the indices of the channel nodes connected directly to the variable node $v_{l,n}$, called its neighborhood, excluding c_t, while the subset of index pairs $\partial t \backslash (l, n)$ stands for the neighborhood of the channel node c_t, excluding $v_{l,n}$.

At the channel node c_t, the conditional probability density function of the received symbol y_t is given by [15]

$$p\left(y_t|\mathbf{v}^{[t]}\right) = \frac{1}{\sqrt{2\pi}\sigma} \exp\left(-\frac{1}{2\sigma^2}\left\|y_t - \mathbf{h}^{[t]T}\mathbf{v}^{[t]}\right\|^2\right), \tag{4}$$

where $\mathbf{v}^{[t]}$ and $\mathbf{h}^{[t]}$ denote the vector containing the symbols overlapped on the tth coupled symbol and their corresponding fraction of effective received signature values, respectively.

Let $LLR_{c_t \to v_{l,n}}$ and $LLR_{v_{l,n} \to c_t}$ be the LLR delivered from the channel node c_t to the variable node $v_{l,n}$ and the LLR from the variable node $v_{l,n}$ to the channel node c_t, respectively. Then we have

$$LLR_{v_{l,n} \to c_t} = \sum_{t' \in \partial(l,n) \backslash t} LLR_{c_{t'} \to v_{l,n}}. \tag{5}$$

where

$$LLR_{c_t \to v_{l,n}} = \log \frac{p_t\left(v_{l,n} = +1 | y_t, \mathbf{v}^{[t]} \backslash v_{l,n}\right)}{p_t\left(v_{l,n} = -1 | y_t, \mathbf{v}^{[t]} \backslash v_{l,n}\right)} \tag{6}$$

$$= \log \frac{p\left(y_t|\mathbf{v}^{[t]}, v_{l,n} = +1\right) p_t\left(\mathbf{v}^{[t]}|v_{l,n} = +1\right)}{p\left(y_t|\mathbf{v}^{[t]}, v_{l,n} = -1\right) p_t\left(\mathbf{v}^{[t]}|v_{l,n} = -1\right)}, \tag{7}$$

Note that (7) is derived from (6) by using Bayes' rule written as

$$p\left(\mathbf{x}|\mathbf{y}\right) = \frac{p\left(\mathbf{y}|\mathbf{x}\right) p\left(\mathbf{x}\right)}{p\left(\mathbf{y}\right)} \propto p\left(\mathbf{y}|\mathbf{x}\right) p\left(\mathbf{x}\right), \tag{8}$$

where the symbol $\propto$ denotes "is proportional to" and the conditional probability density function (pdf) is calculated as

$$p_t\left(\mathbf{v}^{[t]}|v_{l,n}\right) = \prod_{(l',n') \in \partial t \backslash (l,n)} p_t\left(v_{l',n'}\right), \tag{9}$$

with *a priori* probability given by

$$p_t\left(v_{l',n'}\right) = \exp\left(\frac{v_{l',n'}}{2} LLR_{v_{l',n'} \to c_t}\right). \tag{10}$$

Combining (7), (9) and (10), the information of the channel node c_t sent to the variable node $v_{l,n}$ can be written as (12) on the top of the next page, where $\max^*$ operation, is a numerically stable operation suggested in [16].

Outer Iterations Between the Detector and the Decoder. The iterative process between the detector and the decoder is shown as Fig. 4.

In Fig. 4, $LLR_{ext}^{\mathrm{DET}[i]}$ and $LLR_{ext}^{\mathrm{DEC}_l[i]}$, $l \in \{1, 2, \ldots, L\}$ are the output of the detector and L decoders at the ith iteration, respectively, $i = \{1, 2, \ldots, I_{\max}\}$

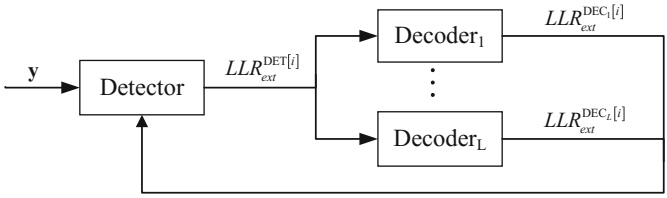

Fig. 4. Block diagram of the iteration between the detector and L decoders.

with $I_{\max}$ defined as the max number of the outer iteration. The subscript "ext" denotes that only the extrinsic information is exchanged during each iteration.

Since we use different encoding scheme in this paper, thus we only focus on the input and output of the decoder in this section, both of which are given as

$$LLR_{ext,v_{l,n}}^{\mathrm{DEC}[i]} = LLR_{v_{l,n}}^{I_{\mathrm{DEC}}} - LLR_{ext,v_{l,n}}^{\mathrm{DET}[i]}, \tag{11}$$

where the left hand side of the equation denotes the output extrinsic information of the decoder at the ith outer iteration. In the right hand side of the equation,

$$\begin{aligned} LLR_{c_t \to v_{l,n}} = & \max_{\substack{\mathbf{v}^{[t]} \\ v_{l,n}=+1}}{}^{*} \left(\sum_{(l',n') \in \partial t \backslash (l,n)} \frac{v_{l',n'}}{2} LLR_{v_{l',n'} \to c_t} - \frac{1}{2\sigma^2} \left\| c_t - \mathbf{h}^{[t]T} \mathbf{v}^{[t]} \right\|^2 \right) \\ & - \max_{\substack{\mathbf{v}^{[t]} \\ v_{l,n}=-1}}{}^{*} \left(\sum_{(l',n') \in \partial t \backslash (l,n)} \frac{v_{l',n'}}{2} LLR_{v_{l',n'} \to c_t} - \frac{1}{2\sigma^2} \left\| c_t - \mathbf{h}^{[t]T} \mathbf{v}^{[t]} \right\|^2 \right) \end{aligned} \tag{12}$$

the minuend is the LLR of the variable node $v_{l,n}$ after I_{DEC} inner iterations of the decoder, which can be used for bit decision. Note that $I_{\mathrm{DEC}} = 1$ for the decoder of convolutional code. The subtrahend denotes *a priori* input information derived from the detector written as

$$LLR_{ext,v_{l,n}}^{\mathrm{DET}[i]} = \sum_{t \in \partial(l,n)} LLR_{c_t \to v_{l,n}}^{I_{\mathrm{DET}}} - LLR_{ext,v_{l,n}}^{\mathrm{DEC}[i-1]}, \tag{13}$$

where $LLR_{c_t \to v_{l,n}}^{I_{\mathrm{DET}}}$ is the soft information sent to the variable node $v_{l,n}$ from its neighborhood channel node c_t after I_{DET} inner iterations of the detector. Note that at the first outer iteration, *a priori* input information received by the detector from the decoders $LLR_{ext,v_{l,n}}^{\mathrm{DEC}[0]}$ is set to be 0 initially.

3.3 EXIT Chart

EXIT chart is a valuable tool to track the mutual information at each iteration between the soft-input soft-output (SISO) constituents, and it gives an excellent visual representation of the process of belief propagation.

To measure the performance of the detector (or the decoder) and determine whether it does produce an increase in mutual information, an input extrinsic information vector is created with the known mutual information I_A and passed into the detector (or the decoder). The detection (or the decoding) algorithm is then employed and the mutual information I_E corresponding to the extrinsic information output by the detector (or the decoder) is calculated. This process is repeated for several different extrinsic information input vectors with different mutual information content, producing corresponding curve in the EXIT chart.

4 EXIT Chart Analysis and Numerical Results

In this paper, we focus on different setup of degree distributions, inner iterations and outer iterations. The system performance can be analysed with the help of EXIT chart.

Generally speaking, with a fixed load, the variable node degree and the channel node degree affect the performance of multiuser detection simultaneously. On the one hand, a higher variable node degree means that each information bit is transmitted in more channel uses, which corresponds to a higher diversity. On the other hand, a higher channel node degree means that there are more transmission bits imposed in one channel use, resulting in a higher interference.

Figure 5 illustrates the EXIT chart over AWGN channel at $E_b/N_0 = 8\,\mathrm{dB}$. For a fair comparison, we keep the modulation load $\alpha = 2$ and the same number of inner iteration $T_{\mathrm{DET}} = 2$ of the detector but varying the degree distribution. It can be seen that as the degrees of variable node and channel node increase, the average mutual information between the transmitted bits and the output

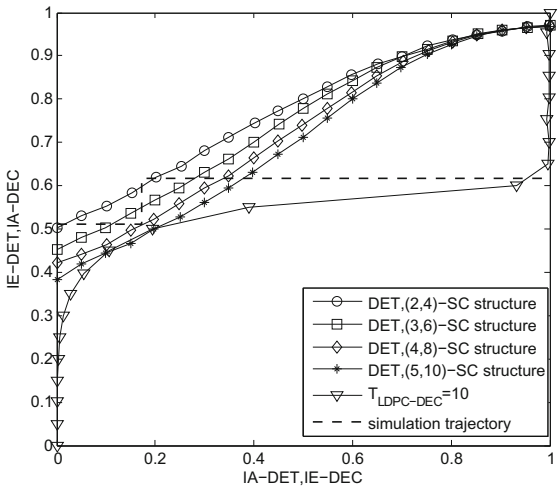

Fig. 5. EXIT chart analysis for detectors with 2 inner iterations for different spatially coupled (SC) structure and the LDPC decoder over AWGN Channel at $E_b/N_0 = 8\,\mathrm{dB}$.

of the detector is reduced, which demonstrates that the interference, instead of diversity, is the dominating factor affecting the performance of the detector. For a fixed load, lower degrees lead to a better performance. The iteration between the detector of a $(2, 4)$-spatially coupled structure and the LDPC decoder is traced in Fig. 5, which is marked by the dashed line.

In the following we study the behavior of the inner iteration within the detector and the decoder respectively. The EXIT curves of the detector for a $(2, 4)$-spatially coupled structure with different number of inner iterations at 6 dB are drawn in Fig. 6. The mutual information between the output of the detector and the transmitted bits increases when allowing more inner iterations of the detector. Moreover, two encoding schemes are considered in the simulation, i.e. convolutional code and LDPC code both with length $N = 1800$ bits and rate $R = 1/2$. Similar to the observation of the detector, the LDPC decoder performs better when there are more inner iterations. The convolutional decoder achieves a better performance than the LDPC decoder with 2 inner iterations, $T_{\mathrm{LDPC-DEC}} = 2$, while it is not as good as the LDPC decoder with $T_{\mathrm{LDPC-DEC}} = 10$ since its output mutual information is smaller than that of the latter when $I_{A-\mathrm{DEC}} > 0.6$. Accordingly, we expect the best BER performance of receivers with the three decoders by using the LDPC decoder with 10 inner iterations.

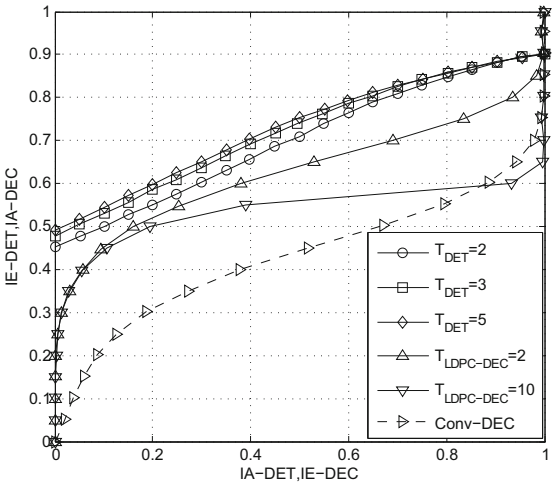

Fig. 6. EXIT chart of detectors with different inner iterations for $(2, 4)$-spatially coupling structure and different decoders over AWGN Channel at $E_b/N_0 = 6$ dB.

The average bit error rates (BER) of all the users' data coupled with $(2, 4)$-matrix is illustrated in Fig. 7. The max number of outer iteration between the detector and the decoder $T_{\max}$ is set to be 20 during the simulation to ensure sufficient iterations at low SNRs. It can be observed that with a fixed decoder, the system achieves better performance as the number of iteration within the

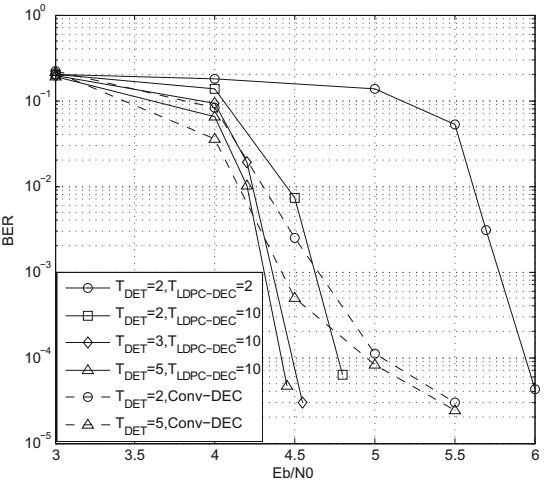

Fig. 7. Average BER performance over AWGN Channel for multiuser data coupled by $(2, 4)$-spatially coupling matrix.

detector T_{DET} increases. Meanwhile, with fixed T_{DET}, the system using the convolutional decoder performs better than using the LDPC decoder with 2 inner iterations, and using the LDPC decoder with 10 inner iterations achieves the best BER performance, which is consistent with the analysis of EXIT chart in Fig. 6.

5 Conclusion

In this paper we consider a signaling format for NOMA system where information is coupled via the superposition of data streams for different users. Each stream is formed by replication and permutation of the encoded bits. An MPA-based iterative detection combining with channel decoding is applied to multiuser detection. The EXIT charts and BER simulation results show that lower node degree of the spatially coupled structure, higher number of iterations of the detector (and the LDPC decoder), and an appropriate encoding/decoding scheme jointly contribute to a better performance of the multiuser transmission system.

References

1. Dai, L., Wang, B., Yuan, Y., Han, S., Chih-Lin, I., Wang, Z.: Non-orthogonal multiple access for 5G: solutions, challenges, opportunities, and future research trends. IEEE Commun. Mag. **53**(9), 74–81 (2015)
2. Chen, S., Peng, K., Jin, H.: A suboptimal scheme for uplink NOMA in 5G systems. In: Wireless Communications and Mobile Computing Conference (IWCMC), Dubrovnik, Croatia (2015)

3. Truhachev, D., Lentmaier, M., Zigangirov, K.S.: Mathematical analysis of iterative decoding of LDPC convolutional codes. In: Proccedings of 2001 IEEE International Symposium on Information Theory, Washington, USA, June 2001
4. Kudekar, S., Richardson, T., Urbanke, R.: Threshold saturation via spatial coupling: why convolutional LDPC ensembles perform so well over the BEC. In: Proceedings of IEEE International Symposium on Information Theory (2010)
5. Kudekar, S., Pfister, H.D.: The effect of spatial coupling on compressive sensing. In: Proceedings of Allerton Conference on Communications, Control, and Computing, Monticello, IL, September 2010
6. Hagiwara, M., Kasai, K., Imai, H., Sakaniwa, K.: Spatially coupled quasi-cyclic quantum LDPC codes. In: Proceedings of IEEE International Symposium on Information Theory, St. Petersburg, Russia (2011)
7. Takeuchi, K., Tanaka, T., Kawabata, T.: Improvement of BP-based CDMA multiuser detection by spatial coupling. In: Proceedings of IEEE Interantional Symposikum on Informationa Theory, St. Petersburg, Russia (2011)
8. Truhachev, D.: Achieving Gaussian multiple access channel capacity with spatially coupled sparse graph multi-user modulation. In: Proceedings of Information Theory and Applications Workshop (ITA), pp. 331–337 (2012)
9. Kschischang, F.R., Frey, B.J., Loeliger, H.-A.: Factor graphs and the sum-product algorithm. IEEE Trans. Inf. Theory **47**(2), 498–519 (2001)
10. Guo, D., Wang, C.-C.: Multiuser detection of sparsely spread CDMA. IEEE J. Sel. Areas Commun. **26**(3), 421–431 (2008)
11. Takeuchi, K., Tanaka, T., Kawabata, T.: Performance improvement of iterative multiuser detection for large sparsely spread CDMA systems by spatial coupling. IEEE Trans. Inf. Theory **61**(4), 1768–1794 (2015)
12. Wen, L., Razavi, R., Imran, M.A., Xiao, P.: Design of joint sparse graph for OFDM system. IEEE Trans. Wirel. Commun. **14**(4), 1823–1836 (2015)
13. Johnson, S.J.: Iterative Error Correction: Turbo, Low-Density Parity-Check and Repeat-Accumulate Codes. Cambridge University Press, New York (2010)
14. Schlegel, C., Burnashev, M., Truhachev, D.: Generalized superposition modulation and iterative demodulation: a capacity investigation. Hindawi J. Electr. Comput. Eng. **2010**, 1 (2010)
15. Hoshyar, R., Wathan, F., Tafazolli, R.: Novel low-density signature for synchronous CDMA systems over AWGN channel. IEEE Trans. Sig. Process. **56**(4), 1616–1626 (2008)
16. Hochwald, B., Brink, S.: Achieving near-capacity on multiple-antenna channel. IEEE Trans. Commun. **51**(3), 389–399 (2003)